Electronic Supplementary Material (ESI) for Physical Chemistry Chemical Physics.
This journal is © the Owner Societies 2021

Electronic Supplementary Information (ESI)

Factors Controlling the Molecular Modification of One-Dimensional Zeolites

Rui Li[1,2]*, William A. Elliott*[3]*, R. John Clark*[2]*, James G. Sutjianto*[2]*, Robert M. Rioux*[3,4*]*, Jeremy C. Palmer*[2*]*, and Jeffrey D. Rimer*[2*]

[1] Beijing Key Laboratory for Green Catalysis and Separation, Department of Environmental Chemical Engineering, Beijing University of Technology, Beijing 100124, PR China

[2] Department of Chemical and Biomolecular Engineering, University of Houston, Houston, TX 77204, USA

[3] Department of Chemical Engineering, The Pennsylvania State University, University Park, PA 16801, USA

[4] Department of Chemistry, The Pennsylvania State University, University Park, PA 16801, USA

*Correspondence sent to: jrimer@central.uh.edu, jcpalmer@uh.edu, and rmr189@psu.edu

Table of Contents

List of Tables and Figures

Methods

Materials. The following chemicals for zeolite synthesis were purchased from Sigma Aldrich (St. Louis, MO): LUDOX AS-30 (30 wt% suspension in water), LUDOX AS-40 (40 wt% suspension in water), potassium hydroxide (85% pellets), aluminum sulfate hydrate (98%, 14-18 H_2O, calculated as $18H_2O$), 1,8-diamonooctane (98%), 1-butanol (99.4%), 1,2-hexanediol (98%), (±)-1,3-butanediol (99%), 1,2,6-hexanetriol (96%), glycerol (99%), ethanol (200 proof), 1,6-hexanediol (99%), 1,2-butanediol (98%), 1,3-propanediol (98%), 1,4-butanediol (99%), spermine (97%), tris(hydroxymethyl)aminomethane (99.7%), L-threonine (98%), L-lysine (97%), 1,2-propanediol (99.5%), ethlyene glycol (98%), and triethylenetetramine (98%). Deionized (DI) water used in all experiments was purified with an Aqua Solutions RODI-C-12A purification system (18.2 MΩ). All reagents were used as received without further purification.

Zeolite Crystallization. ZSM-22 zeolites were synthesized with 1,8-diamonooctane (C_8DN) as an organic structure-directing agent (OSDA). Growth solutions were prepared with a molar composition of 1 Al_2O_3: 90 SiO_2:11.9 K_2O: 27.3 C_8DN: 3588 H_2O.[1] In a typical synthesis, solutions of each component were prepared separately: KOH solution was prepared by dissolving potassium hydroxide (0.21 g) in DI water (0.91 g); aluminium solution was made by dissolving aluminium sulfate (0.089 g) in DI water (0.91 g); C_8DN (0.53 g) was dissolved in DI water (3.64 g); and LUDOX AS-30 (2.37 g) mixed with DI water (1.35 g) was introduced as a colloidal suspension. The KOH, OSDA, and $Al_2(SO_4)_3$ solutions were first mixed together and stirred for ca. 5 min to generate a uniform mixture. The silica suspension was then added dropwise under constant stirring. The resulting mixture was left to stir overnight (ca. 21 h) at room temperature (referred to herein as the "aging" period). After aging was complete, the growth mixture (ca. 10 g) was placed in a Teflon-lined stainless steel acid digestion bomb (Parr Instruments) and was heated under rotation at 34 rpm in a ThermoFisher Precision Premium 3050 Series gravity oven at 160°C and autogenous pressure. ZSM-22 growth mixtures and the resulting crystals prepared by this procedure (in the absence of modifier) are referred to as the *control.*

Zeolite L was synthesized in the absence of an organic using K^+ as an inorganic structure-directing agent (SDA). Growth mixtures were prepared with a molar ratio of 0.5 Al_2O_3:20 SiO_2:10.2 K_2O:1030 H_2O according to a reported protocol.[2] Potassium hydroxide (0.64 g) was first dissolved in DI water (7.78 g), followed by the addition of aluminium sulfate (0.17 g). This mixture was stirred until clear (*ca.* 5 min). LUDOX AS-40 (1.42 g) was added and the resulting mixture was aged overnight (ca. 21 h) with constant stirring. The aged growth mixture (ca. 10 g) was placed in a Teflon-lined stainless steel acid digestion bomb and was heated under static conditions at 180°C and autogenous pressure. Zeolite L growth mixtures and the resulting crystals prepared by this procedure are referred to as the *control.*

In select cases, a zeolite growth modifier (ZGM) was added 2 h prior to the finish of the aging period (ca. 19 h). Alcohols were added in a molar ratio of 1.5 ZGM:1.0 SiO_2 while amines and amino acids were employed as 1 wt% of the entire growth mixture (unless otherwise specified). The pH of the growth mixture was measured with a Thermo Scientific Orion 3 Star meter. The ionic conductivity of the solution was measured with a VWR international EC meter (Model 2052). For diffraction and microscopy analyses, solids in the growth mixture were isolated as a white powder (ca. 1 g) by centrifugation at 13,000 rpm for 45 min. The solid was washed with DI water to remove the supernatant. The centrifuge-wash cycle was repeated for a second time and the resulting gel was dried at ambient conditions. During the preparation of microscopy samples, an aliquot of the sample suspension was placed on a glass slide and dried overnight. Crystals on the glass slide were transferred to SEM sample holders (Ted Pella) by gently pressing the glass slide on carbon tape.

Materials Characterization. Solids extracted from a zeolite growth mixture were characterized by powder X-ray diffraction (XRD) using a Rigaku SmartLab Diffractometer with Cu-Kα radiation (40 kV, 44 mA, 1.54 Å). Scanning electron microscopy (SEM) was performed with a FEI 235 Dual-Beam (Focused Ion-beam) or a LEO 1525 FEG system operated at 15 kV and a 5-mm working distance. All SEM samples were coated with a thin layer of carbon (ca. 30 nm) prior to imaging. The average size and size distribution of crystals in each batch were obtained from at least 100 measurements performed on SEM images. Thermogravimetric analysis (TGA) was performed with a SDT Q600 V8.3 thermogravimetric analyzer (TA Instruments) using a heating rate of 1 °C min^{-1} and 100 mL min^{-1} air flow. The temperature was raised from 25 to 545°C where it held for 10 h before raising the temperature from 545 to 800°C.

Calorimetry Studies. Calorimetry measurements were made on a semi-adiabatic solution calorimeter (TAMIII Precision Solution Calorimeter, TA Instruments) maintained at 25.0000 ± 0.0001°C. The zeolite was dried under flow of helium at 400°C for 4 h with a ramp rate of 2 °C/min. The zeolite was stored under nitrogen to prevent uptake of atmospheric moisture. Zeolite powder (20 mg) was placed in a 1 mL glass ampoule and sealed with a silicone rubber stopper and beeswax. The ampoule was submerged in a 25 mL reaction vessel containing the wetting solution. The ampoule was broken while stirring at 600 rpm and the change in temperature associated with the wetting event was measured. The heat capacity of the system was determined by injecting a pulse of 3 J before and after breaking the ampoule. The temperature change was converted to enthalpy change using the average of the heat capacities. An empty ampoule was broken in each solution to determine the heat associated with the breaking of the ampoule. This was used to correct the raw heat for the true heat of wetting. SolCal software (v1.2, TA Instruments) was used to analyze the experimental data. An image of the solution calorimeter cell and experimental data is shown in Fig. S5.

Molecular Modeling. Molecular dynamics (MD) simulations were performed using GROMACS 4.6.7 [3] to study the adsorption of selected ZGMs (1,2-butanediol ($D4_{1,2}$), 1,3-butanediol ($D4_{1,3}$) and 1,4-butanediol ($D4_{1,4}$)) on the crystallographic surfaces of an all-silica **TON** zeolite structure. The ZGMs were modeled using the generalized AMBER force field[4], whereas the zeolite framework was described with the ClayFF potential.[5] Force field parameters for modeling van der Waals interactions between the ZGMs and the zeolite framework were determined using standard Lorentz-Berthelot combining rules. Real-space van der Waals and Coulombic interactions were truncated using a cutoff of 0.9 nm. Long-range contributions to the electrostatic interactions were treated using the particle mesh Ewald method, with parameters chosen to ensure a relative error of less than 10^{-5} in the calculated energy. The equations of motion were integrated using a leap-frog scheme with a 2 fs time step, and temperature was maintained using a Bussi-Parrinello[6] velocity-rescaling thermostat with a 2 ps relaxation time constant.

The model of **TON** was constructed from unit cell data (lattice parameters and atomic positions) reported in the International Zeolite Association's Database of Zeolite Structures. The unit cells from the database were replicated to generate a 3 × 2 × 7 supercell for **TON**. Model surfaces were created from the supercells by disrupting its periodicity along the axes perpendicular to the crystallographic planes of interest. In each case, the position at which the periodicity was disrupted was chosen to minimize the number of broken Si-O bonds and hence the surface energy. Following Kroutil et al.,[7] approximately 80% of the undercoordinated oxygens were protonated on each surface and the charges assigned to non-surface oxygens within the zeolite framework were adjusted slightly (<0.1) to compensate for excess surface charge and ensure electroneutrality.

The MD simulations of each zeolite surface were performed using an infinite slab geometry. The infinite slabs were generated by placing each model zeolite surface in an elongated rectangular simulation cell with its surface normal aligned parallel to the cell's major axis (z-axis). The dimensions of the simulation along the minor axes (x- and y-axes) were chosen to be commensurate with the periodicity of the zeolite structure, whereas the length of major axis was chosen to be at least three times larger than the thickness of the zeolite slab. A single ZGM molecule was placed in the empty region above the slab's upper surface and the system was solvated with $\sim$5000 SPC/E [8] water molecules to create two solid-liquid interfaces. The solvated system was then equilibrated for 10 ns in the isothermal-isobaric ensemble at 300 K and 1 bar using an anisotropic Parrinello-Rahman barostat [9] with a 2 ps relaxation time constant to impose constant pressure (isostress) conditions along the z-axis of the simulation cell.

Modifier adsorption on **TON** was characterized by computing the potential of mean force (PMF) $W(d_{\text{com}}) = -k_{\text{B}}T\ln[P(d_{\text{com}})]$, where d_{com} is the separation distance along the z-axis of the simulation cell between the ZGM's center of mass and the zeolite surface, k_{B} is the Boltzmann constant, T is the temperature, and $P(d_{\mathrm{com}})$, is the equilibrium density distribution associated with d_{com}. The binding energy from solution was estimated from the PMF using $\Delta F_b \approx W(d_{\mathrm{b}}) - W(d_{\mathrm{u}})$, where d_{b} and d_{u}, correspond to the characteristic separation distances for the bound and unbound states of the ZGM, respectively. Accurate estimates of $P(d_{\mathrm{com}})$ were obtained for each ZGM by performing windowed umbrella sampling MD (USMD) simulations using the PLUMED 2.1.1 plugin [10] for GROMACS. The USMD simulations were carried out in the canonical ensemble at 300 K, with the z-dimension of the simulation box fixed to the average value computed from the isothermal-isobaric simulations described above. Independent USMD simulations were run in each sampling window using a harmonic bias potential with a spring constant $k = 750\ \mathrm{kJ\ mol^{-1} nm^{-2}}$ to restrict sampling to the targeted region along d_{com}. A window spacing of 0.05 nm was chosen to ensure sufficient statistical overlap between the sampled distributions in adjacent regions. Each simulation was equilibrated for at least 2 ns, followed by a production period of ~ 10 ns. Data from the production period of each USMD simulation were combined using BayesWHAM [11] to obtain an unbiased global estimate of the PMF.

Supporting Text

Molar heats of wetting from solution calorimetry data

The data presented in Fig. 3 and 4 represent the observed heat of wetting per gram of zeolite (**LTL** or **TON**). A known amount of zeolite was carefully weighed after drying and loaded into a 1 mL ampoule and then sealed. The ampoule preparation process occurred in a glovebox to ensure the zeolite remained dry. After breaking the ampoule, allowing the surrounding solution to fill into the ampoule, the measured heat is inclusive of all chemical interactions occurring between the solution components and the zeolite powder. Zeolites were completely wetted by the solution and remained suspended in solution due to stirrring. We did not experience any accumulation of zeolite at the solution-air interface. The measured heat was normalized per gram of dry zeolite powder added to the ampoule. It is common practice to report heats of wetting on per gram basis, since the exact amount of solute adsorbed/absorbed is unknown. An additional method that quantifies the amount of solute absorbed and/or adsorbed is required; adsorption isotherms generally satisfy this requirement since dilute solute is adsorbed from the bulk solution and a mass balance can be used to determine the amount absorbed or adsorbed (i.e, total amount of solute sorbed). This difference makes it challenging to transform an enthalpy per gram solid to a value per mole of solute. In a wetting experiment, the calorimeter collects heat flow data that is inclusive of not only solute sorption, but also solvent sorption and other factors. From liquid-phase adsorption isotherms, the total amount of solute adsorbed is the only quantity recovered since solids are pre-wetted with solvent before solute introduction.

Since we do not have adsorption isotherm data at the solution conditions utilized here, we surveyed the literature and extracted values for equilibrium constants for alcohol(s) and diol(s) sorption from aqueous solutions in zeolites.[12-15] We were unable to find any references on alcohol or diol sorption from aqueous solution into **LTL** or **TON** zeolites; but since **MOR** and **MFI** zeolites are structurally similar to **LTL** and **TON**, respectively, we additionally searched for references on **MOR** and **MFI**. Our literature search only turned up references for alcohol and diol sorption from aqueous solution into **MFI**. We were able to find adsorption from aqueous solution data for ethanol, 1-butanol, 1,2-butanediol, glycerol, and ethylene glycol, but no data could be found for 1,3-butanediol or 1,4-butanediol. Overall, these data should be considered carefully, and only compared to **TON**.

Units of K_{ads}. The adsorption constants are reported (or were converted) into units of [mL solution/g zeolite]. Adsorption constants were either reported in the original reference or we calculated adsorption constants from reported uptake versus concentration data. Calculated values were determined by the analysis of adsorption data (alcohol adsorbed vs. final solution concentration) as [mol alcohol adsorbed/g zeolite] versus [mol alcohol/mL solution] or on a weight basis as [g alcohol adsorbed/g zeolite] versus [g alcohol/mL solution]. Molecular weight and density values at room temperature of the neat alcohol or diol was used to convert units.

Data processing procedure. These calculations carried out in a Microsoft Excel spreadsheet. The spreadsheet is available from RMR. First, the initial concentration of the alcohol in the solution is determined. Second, the amount of alcohol sorbed by the zeolite is determined using the initial alcohol concentration and adsorption constant. Finally, the molar adsorption enthalpy is calculated from the experimentally determined heat of wetting (per mass of zeolite) and amount of alcohol sorbed by the zeolite.

Assumption 1: All observed heat from wetting is due to the sorption of alcohol. Sorption is inclusive of adsorption and absorption.

Assumption 2: Change in bulk solution volume is unchanged by liquid uptake in the zeolite. This assumption is made based on the small amount of zeolite (~0.02 g) compared to amount of solution (25.75 g).

Assumption 3: Volumes of liquids are additive. The total volume of solution is the sum of volumes of alcohol and KOH solution (i.e., we assume ideal solution behavior with a negligible excess molar volume, $V_{\text{excess}} = 0$).

Calculations. The first step is to determine the initial concentration of alcohol. Here assumption 3 is considered. The total volume of solution is the sum of the volume of 0.1 M KOH solution (25 mL) and the volume of alcohol.

$$c_{A,i} = \frac{n_A}{V_t} = \frac{(m_A/M_A)}{V_{KOH}+V_A} \tag{S1}$$

where *n* is the moles of alcohol (or diol) A, *V* is volume, *c* is concentration, *m* is mass, *M* is molar mass, and subscript *i* represents an initial quantity (with *t* denoting the total of a quantity).

The second step is to determine the number of moles of alcohol adsorbed. Here we utilize assumption 2. We do not assume the concentration of alcohol remains constant in the bulk solution, i.e. we assume the amount of alcohol taken up is non-negligible relative to amount of alcohol in bulk; however, the amount of alcohol sorbed by the zeolite is ultimately negligible relative to the amount of alcohol in the bulk.

We first consider the equation for the adsorption constant (assuming we are in the Henry's regime), K_{ads}. In this case, the subscript *ads* is inclusive of both absorption and adsorption.

$$K_{ads} = \frac{(n_{A,ads}/m_z)}{c_{A,f}} \tag{S2}$$

Substituting in $c_{A,f} = \frac{n_{A,f}}{V_t}$ where *f* represents a final quantity

$$K_{ads} = \frac{(n_{A,ads}/m_z)}{(n_{A,f}/V_t)} \tag{S3}$$

with $n_{A,f} = n_{A,t} - n_{A,ads}$ and $V_t = V_{KOH} + V_A$, K_{ads} becomes

$$K_{ads} = \frac{(n_{A,ads}/m_z)}{\frac{n_{A,t}-n_{A,ads}}{V_{KOH}+V_A}} \tag{S4}$$

And recognizing $n_{A,t} = c_{A,i}(V_{KOH} + V_A)$, K_{ads} becomes

$$K_{ads} = \frac{(n_{A,ads}/m_z)}{\frac{c_{A,i}(V_{KOH}+V_A)-n_{A,ads}}{V_{KOH}+V_A}} \tag{S5}$$

Solving for $n_{A,ads}$

$$n_{A,ads} = \frac{c_{A,i}(V_{KOH}+V_A)K_{ads}m_Z}{K_{ads}m_Z+V_{KOH}+V_A} \tag{S6}$$

Normalizing by mass of zeolite

$$\frac{n_{A,ads}}{m_z} = \frac{c_{A,i}(V_{KOH}+V_A)K_{ads}}{K_{ads}m_Z+V_{KOH}+V_A} \tag{S7}$$

where the subscript *z* refers to the zeolite. Finally, we calculate the molar adsorption of the alcohol under assumption 1,

$$\Delta H_{ads} = \frac{\Delta H_{wet}}{(n_{A,ads}/m_z)} \tag{S8}$$

where ΔH_{ads} is the molar heat of adsorption and ΔH_{wet} is the heat of wetting (per mass of zeolite).

Molar heat of adsorption calculations. The results for the conversion of ΔH_{wet} to ΔH_{ads} (where "ads" is inclusive of both absorption and adsorption) are summarized in Table S7. It is evident that some of the results for ΔH_{ads} for certain alcohols or diols provide reasonable values for molar heats of adsorption, while several calculated values are obviously incorrect. There are several reasons that may lead to the noted discrepancies. The relevant data found in the literature are for **MFI** framework since no data could be found for **TON** or **LTL**. Based on their similar topology, we used the available literature data for **MFI** to approximate for **TON**. Fig. 3 and 4 demonstrate the heat of wetting values measured with solution calorimetry are consistent and within error on the control sample (i.e., alkaline KOH solution with no alcohol added). From the heat of wetting data, there appears to be only a 10 J/g difference for the various alcohols over **TON** and **LTL**, but from analysis of the published data summarized in Table S7, the values for K_{ads} across the same catalyst, H-ZSM-5 (Zeolyst CBV28014, Si/Al = 140) for different alcohols varies considerably (K_{ads} (in mL/g): 107 for 1,2-butanediol; 1.73 for ethylene glycol; and 0.7 for glycerol at 278 K). Additionally, the compiled data demonstrates for the same alcohol (1,2-butanediol), the measured adsorption equilibrium constant for silicate-1 (**MFI** with Si/Al = ∞) varies from to 10 to 225 mL/g. In this case, the SiOH density varied amongst the silicate-1 samples and considered important to K_{ads}. It is apparent from the limited number of studies found in the literature, both the properties of the zeolite and identity of the alcohol impact the measured equilibrium adsorption constant that is "washed out" in the alkaline solution used here. The conditions at which the dilute solute was adsorbed from aqueous solution from literature reports varied significantly in terms of pH, ionic strength, and potential competitive adsorption (e.g. K^+ and OH^-). This is the most likely reason for the insensitivity of ΔH_{wet} on the type of alcohol on **TON** (and **LTL**).

Supporting Tables

Table S1. Synthesis parameters and references for the **LTL** and **TON** phase diagram in Fig. S1.

References	Molar ratio			Molar fraction			T (°C)	Time (h)	Phase	Cation
	x Si	y Al	z H_2O	Si	Al	OH^-				
Jamil et al. (2016)[16]	91	2	3202	0.62	0.01	0.36	180	48-96	TON	K^+
Wang et al. (2016)[17]	1	0	44	0.84	0.02	0.14	150	48	TON	K^+
Hogan et al. (1984)[18]	30	2	1500	0.68	0.05	0.27	180	64	TON	K^+
Hogan et al. (1984)[18]	95	1	3600	0.94	0.02	0.05	150	84	TON	Na^+
Hogan et al. (1984)[18]	60	2	2500	0.88	0.03	0.09	180	216	TON	Cs^+
Hogan et al. (1984)[18]	170	2	8000	0.85	0.01	0.14	180	192	TON	Rb^+
Parker and Bibby (1983)[19]	0	0	1	0.70	0.01	0.29	150	NA	TON	Na^+
Parker and Bibby (1983)[19]	0	0	1	0.71	0.00	0.29	150	NA	TON	Na^+
Parker and Bibby (1983)[19]	0	0	1	0.69	0.03	0.28	150	NA	TON	Na^+
Araya and Lowe (1984)[20]	60	1	3000	0.85	0.01	0.14	180	14	TON	K^+
Asensi et al. (1998)[21]	124	1	5966	0.63	0.01	0.37	160	24	TON	Na^+
Asensi et al. (1998)[21]	28	1	1440	0.55	0.02	0.43	160	24	TON	Na^+
Asensi et al. (1998)[21]	27	1	1512	0.62	0.02	0.36	160	24	TON	Na^+
Ernst et al. (1989)[22]	91	2	3670	0.76	0.02	0.22	160	48	TON	K^+
Olson et al. (1984)[23]	90	2	3600	0.82	0.02	0.16	160	48	TON	K^+
Olson et al. (1984)[23]	180	2	7200	0.90	0.01	0.09	160	71	TON	Na^+
Jamil et al. (2014)[24]	91	2	3202	0.62	0.01	0.36	180	12	TON	Na^+
Lowe et al. (1983)[25]	60	2	3000	0.83	0.03	0.14	180	49	TON	Rb^+
Lowe et al. (1983)[25]	60	0	3000	0.85	0.00	0.14	180	NA	TON	K^+
Wang et al. (2014)[26]	1	0	45	0.81	0.02	0.18	140	48	TON	K^+
Valyocsik (1984)[27]	100	0	4000	0.77	0.00	0.23	160	48	TON	K^+
Valyocsik (1984)[27]	100	3	4000	0.75	0.03	0.22	160	72	TON	K^+
Ball et al. (1985)[28]	77	2	975	0.91	0.02	0.07	170	48	TON	Na^+
Gaona-Gómez and Cheng (2012)[29]	20	2	1030	0.46	0.05	0.50	180	72	LTL	K^+
Larlus and Valtchev (2004)[30]	1	0.2	15	0.60	0.10	0.30	170	72	LTL	K^+
Megelski and Calzaferri (2001)[31]	11	2	169	0.57	0.11	0.32	160	144	LTL	K^+
Megelski and Calzaferri (2001)[31]	10	2	161	0.58	0.12	0.30	160	144	LTL	K^+
Trakarnroek et al. (2006)[32]	10	1	160	0.62	0.06	0.32	170	96	LTL	K^+
Trakarnroek et al. (2006)[32]	9	2	164	0.58	0.13	0.29	175	96	LTL	K^+
Trakarnroek et al. (2006)[32]	10	2	160	0.53	0.11	0.37	150	120	LTL	K^+
Trakarnroek et al. (2006)[32]	10	2	400	0.31	0.06	0.63	175	8	LTL	K^+
Huo et al. (2010)[33]	1	0	25	0.67	0.13	0.2	150	4	LTL	K^+
Jentoft et al. (2006)[34]	25	2	400	0.53	0.04	0.43	NA	NA	LTL	K^+
Itani et al. (2011)[35]	1	0	20	0.48	0.05	0.48	170	24	LTL	K^+
Itani et al. (2011)[35]	1	0	16	0.56	0.1	0.34	160	20	LTL	K^+

Table S2. ZGMs screened for zeolite ZSM-22 and average size and AR of crystalline products.

	ZGM Name	Fomula	MW(gmol^{-1})	Structure	Average width/nm	Aspect ratio (L/D)
	Control				105.73	5.47
Alcohols	Ethanol	C_2H_6O	46.07	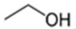	178.64	7.35
	Ethylene glycol	$C_2H_6O_2$	62.07	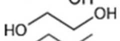	132.04	4.31
	1,2-Propanediol	$C_3H_8O_2$	76.09	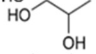	188.59	5.83
	1,3-Propanediol	$C_3H_8O_2$	76.09		112.39	6.17
	1-Butanol	$C_4H_{10}O$	74.12	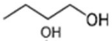	132.85	8.00
	1,2-Butanediol	$C_4H_{10}O_2$	90.12	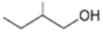	131.89	5.90
	1,4-Butanediol	$C_4H_{10}O_2$	90.12	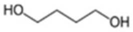	128.72	8.43
	1,3-Butanediol	$C_4H_{10}O_2$	90.12	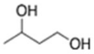	135.40	10.02
	1,6-Hexanediol	$C_6H_{14}O_2$	118.17	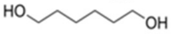	130.51	7.85
	1,2-Hexanediol	$C_6H_{14}O_2$	118.17	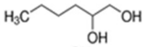	125.23	6.44
	Glycerol	$C_3H_8O_3$	92.09	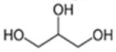	97.90	8.39
	1,2,6-Hexanetriol	$C_6H_{14}O_3$	134.17	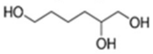	127.12	7.76
Amines	TETA	$C_6H_{18}N_4$	146.23	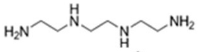	154.24	4.92
	L-Lysine	$C_6H_{14}N_2O_2$	146.19	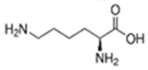	143.48	8.47
	L-Threonine	$C_4H_9NO_3$	119.12	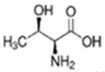	134.71	7.29
	Spermine	$C_{10}H_{26}N_4$	202.34	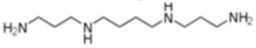	157.94	4.40
	THAM	$C_4H_{11}NO_3$	121.14		119.63	5.02

Table S3. Parametric study of zeolite ZSM-22 syntheses.

Sample	DAO: SiO_2	K_2O: SiO_2	H_2O: SiO_2	Synthesis	T (°C)	Time (d)	Zeolite
N-1	0.3	0.13	40	Rotation	160	3	TON
N-2	0.3	0.13	40	Rotation	160	14	TON
N-3	0.3	0.17	40	Rotation	160	3	MEL
N-4	0.3	0.13	40	Static	180	3	MEL
N-5	0.3	0.04	40	Static	160	3	Amorphous
N-6	0.3	0.04	40	Static	160	14	MEL
N-7	0.3	0.04	40	Static	160	31	MEL
N-8	0.3	0.03	40	Static	160	7	Amorphous
N-9	0.3	0.03	40	Static	160	14	MEL
N-10	0.3	0.03	40	Static	160	31	MEL
N-11	0.3	0.13	11	Rotation	160	3	MEL + TON
N-12[a]	0.3	0.13	40	Rotation	160	1	Amorphous
N-13[a]	0.3	0.13	40	Rotation	160	3	MEL
N-14[b]	0.3	0.13	40	Rotation	160	3	Amorphous
N-15[c]	0.3	0.13	40	Rotation	160	3	TON
N-16[d]	0.3	0.13	40	Static	160	3	TON + MEL
N-17[e]	0.3	0.13	40	Rotation	160	3	TON
N-18[d,e]	0.3	0.13	40	Static	160	3	MEL

[a] synthesized with alternative Si source Ludox SM-30; [b] synthesized with alternative Si source potassium silicate; [c] rotation until the end of induction time (i.e., 17 h) then static to 3 d; [d] static for 17 h then rotation to 3 d; [e] synthesized with alternative Si source Syton HT-50

Table S4. Raw calorimetry data of zeolite L crystals adsorbing selected ZGMs in basic aqueous solutions.

ZGM name	Mass of zeolite (mg)	Measured net heat (J)	Heat of wetting (J/g)	Average heat (J/g)	Standard deviation (J/g)
No ZGM (0.1M KOH solution)	21.5	-1.8	-84.8	-83.7	0.9
	20.5	-1.7	-83.6		
	21.7	-1.8	-82.6		
Ethanol (P2)	20.7	-1.7	-83.4	-84.2	0.6
	21.5	-1.8	-84.9		
	22.9	-1.9	-84.4		
Butanol (P4)	20.7	-1.8	-86.1	-85.8	0.2
	23.5	-2.0	-85.8		
	21.2	-1.8	-85.6		
Ethylene glycol ($D2_{1,2}$)	22.1	-1.9	-85.1	-86.1	0.9
	23.2	-2.0	-87.3		
	20.6	-1.8	-85.9		
1,2-Butanediol ($D4_{1,2}$)	19.8	-1.7	-85.1	-84.7	0.3
	20.1	-1.7	-84.4		
	22.7	-1.9	-84.5		
1,3-Butanediol ($D4_{1,3}$)	21.2	-1.8	-86.8	-85.6	0.9
	19.8	-1.7	-85.3		
	21.1	-1.8	-84.6		
1,4-Butanediol ($D4_{1,4}$)	19.0	-1.6	-84.8	-83.9	0.7
	20.9	-1.8	-83.9		
	18.9	-1.6	-83.1		
Glycerol ($T3_{1,2,3}$)	23.9	-2.0	-85.6	-84.9	0.5
	21.7	-1.8	-84.3		
	20.7	-1.8	-85.0		

Table S5. Raw calorimetry data of ZSM-22 crystals adsorbing selected ZGMs in basic aqueous solutions.

ZGM name	Heat of wetting (J/g)	Average heat (J/g)	Standard deviation (J/g)
No ZGM (0.1M KOH solution)	-53.9 -53.2 -54.9	-54.0	0.9
Ethanol (P2)	-58.6 -56.2 -54.3 -55.4 -60.4 -60.9 -59.7	-57.9	2.6
Glycerol ($T3_{1,2,3}$)	-45.6 -44.9 -49.0 -49.8 -46.8 -52.6 -52.3	-48.7	3.1
Ethylene glycol ($D2_{1,2}$)	-55.9 -56.5 -56.0	-56.1	0.3
Butanol (P4)	-50.3 -50.0 -51.4 -54.4 -56.6 -57.7	-53.4	3.3
1,2-Butanediol ($D4_{1,2}$)	-49.6 -51.7 -51.7 -54.3 -55.4 -53.2	-52.6	2.1

Table S5 continued…

ZGM name	**Heat of wetting (J/g)**	**Average heat (J/g)**	**Standard deviation (J/g)**
1,3-Butanediol ($D4_{1,3}$)	-48.5	-52.2	3.1
	-48.3		
	-53.9		
	-55.8		
	-53.8		
	-52.9		
1,4-Butanediol ($D4_{1,4)}$	-56.9	-58.0	0.8
	-58.6		
	-58.4		

Table S6. Literature summary of reported adsorption equilibrium isotherm data for alkanol (alcohols, diols, triols) from aqueous solution. All zeolites are MFI.

Description	**Si/Al ratio**	**Cation**	**Alcohol**[a]	**T (K)**	**K_{ads} ($mL_{soln}/g_{zeolite}$)**[b]	**Ref**	**Sorbed amount (mmol/g)**[c,d]	**ΔH_{wet} (J/g)**[e]	**ΔH_{ads} (kJ/mol)**
CBV28014 (H-ZSM-5)	140	H	1,2-BD	278	107	[12]	31.2	-52.6	-2
Silicalite-1	∞	--	1,2-BD	298	29.3	[13]	9.1	-52.6	-6
silicalite-1 – alkaline – SiOH/uc = 8.5	∞	--	1,2-BD	298	225	[14]	60.7	-52.6	-1
silicalite-1 – alkaline – SiOH/uc = 3.9	∞	--	1,2-BD	298	86.2	[14]	25.6	-52.6	-2
silicalite-1 – alkaline – SiOH/uc = 2.9	∞	--	1,2-BD	298	75.7	[14]	22.6	-52.6	-2
silicalite-1 – alkaline – SiOH/uc = 0	∞	--	1,2-BD	298	9.1	[14]	2.9	-52.6	-19
silicalite-1	∞	--	1,2-BD	298	26	[15]	8.1	-52.6	-7
silicalite-1	∞	--	1-butanol	298	850	[15]	199.6	-53.4	-0.3
silicalite-1	∞	--	ethanol	298	12	[15]	7.4	-57.9	-8
CBV28014 (H-ZSM-5)	140	H	EG	278	1.7	[12]	0.8	-56.1	-71
silicalite-1	∞	--	EG	298	1.6	[13]	0.7	-56.1	-77
silicalite-1 – alkaline – SiOH/uc = 8.5	∞	--	EG	298	1.8	[14]	0.8	-56.1	-68
silicalite-1 – alkaline – SiOH/uc = 3.9	∞	--	EG	298	0.75	[14]	0.3	-56.1	-166
silicalite-1 – alkaline – SiOH/uc = 2.9	∞	--	EG	298	0.5	[14]	0.2	-56.1	-256
silicalite-1 – alkaline – SiOH/uc = 0	∞	--	EG	298	0.05	[14]	0.0	-56.1	-2460
silicalite-1	∞	--	EG	298	1.4	[15]	0.6	-56.1	-88
CBV28014 (H-ZSM-5)	140	H	glycerol	278	0.7	[12]	0.2	-48.7	-222
silicalite-1	∞	--	glycerol	298	1.3	[13]	0.4	-48.7	-127
silicalite-1	∞	--	glycerol	298	1.3	[15]	0.4	-48.7	-123

[a] 1,2-BD = 1,2-butanediol. EG = ethylene glycol

[b] The reported (or calculated) equilibrium adsorption constant in units of $mL_{soln}/g_{zeolite}$ was used to calculate the amount of alcohol sorbed during the solution calorimetry experiments reported in this work.

[c] The molecular weight (g/mol) and density (g/mL) were used to calculate the uptake of each alkanol. The molecular weight and density of 1,2-BD are 90.12 and 1.006; 74.12 and 0.81 for 1-butanol; 46.07 and 0.79 for ethanol; 62.07 and 1.11 for EG; 92.09 and 1.261 for glycerol.

[d] Solution calorimetry experiments in this work employed 20 mg zeolite, 0.75 g of alkanol, and 25 mL of 0.1M KOH solution.

[e] Average heat of wetting value from Table S5.

Table S7. Simulation results of modifier adsorption on other surfaces of ZSM-22.

	Surface binding energies (kJ/mol) [a]		
ZGM	**(001) face**	**(010) face**	**(100) face**
1,2-Butanediol ($D4_{1,2}$)	-2.2	-1.9	-1.2
1,3-Butanediol ($D4_{1,3}$)	-1.5	-2.1	-1.3
1,4-Butanediol ($D4_{1,4)}$	-0.5	-4.2	-0.2

a. Estimated uncertainties are less than 0.5 kJ/mol

Supporting Figures

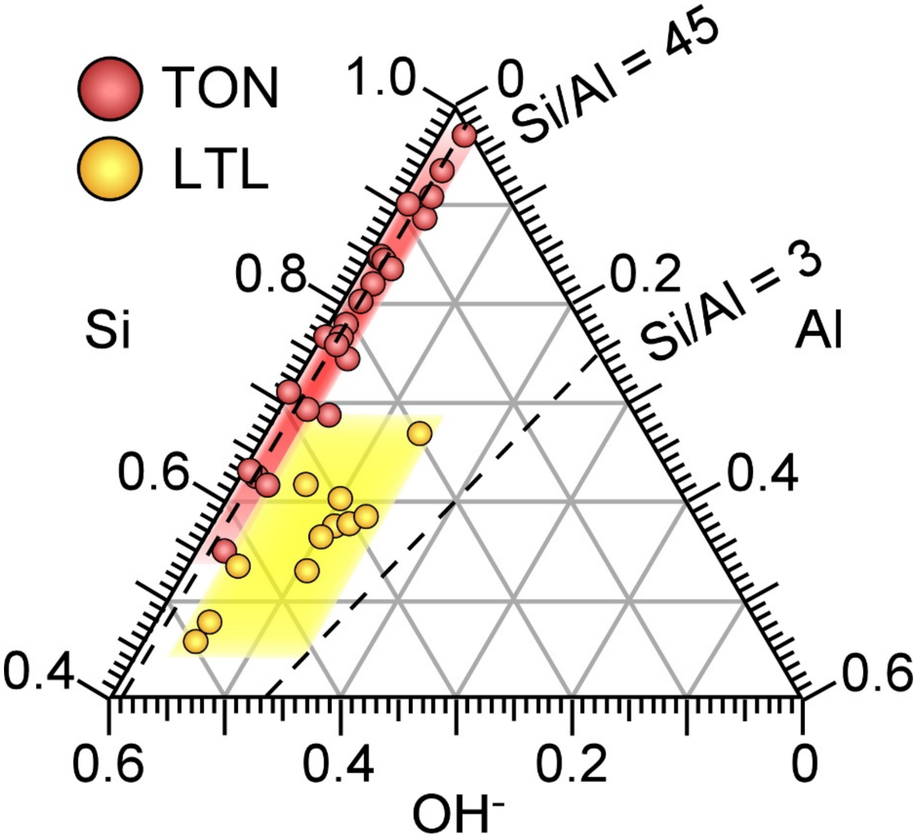

Fig. S1 Ternary (kinetic) phase diagram based on growth conditions listed in Table S1 for the synthesis of zeolite L (yellow) and ZSM-22 (red).

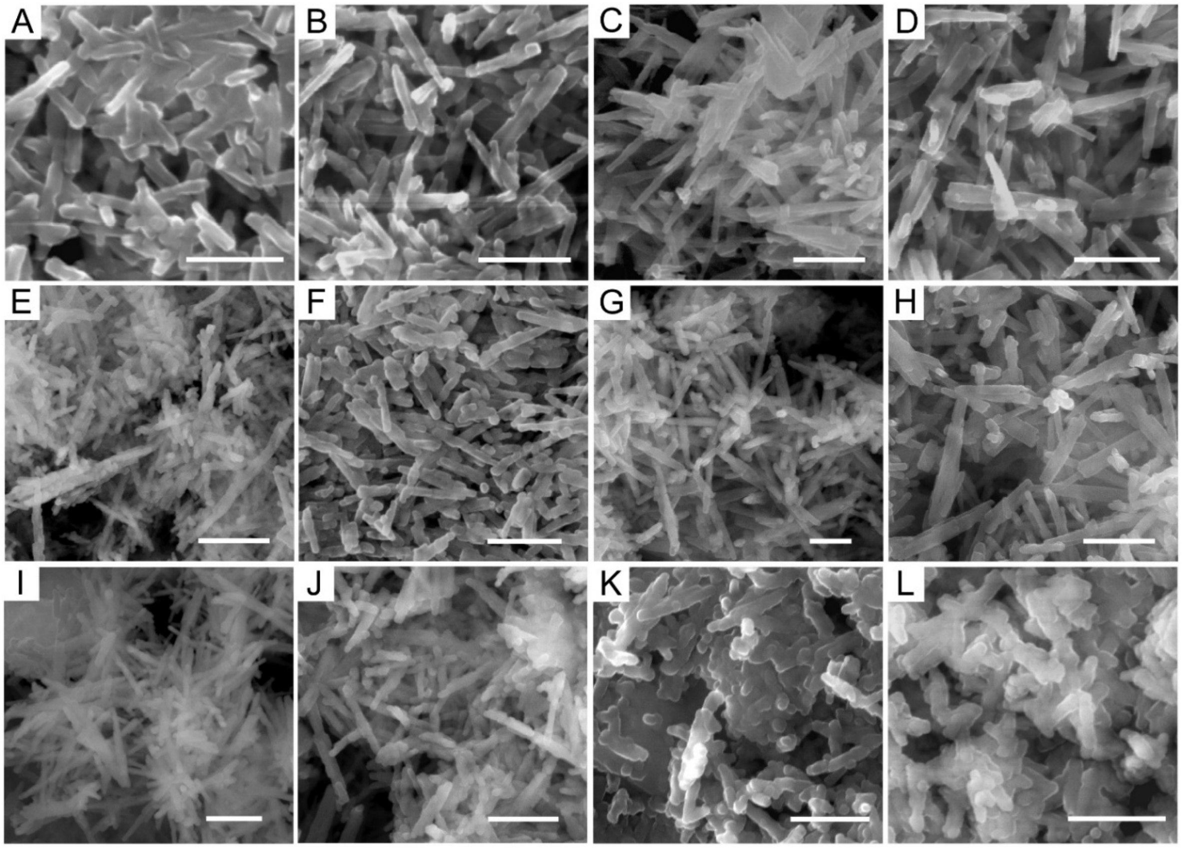

Fig. S2 Scanning electron micrographs of ZSM-22 crystals modified using selected ZGMs: (A) ethylene glycol ($D2_{1,2}$), (B) 1,2-butanediol ($D4_{1,2}$), (C) 1,4-butanediol ($D4_{1,4}$), (D) 1,6-hexanediol ($D6_{1,6}$), (E) glycerol ($T3_{1,2,3}$), (F) 1,2,6-hexanetriol ($T6_{1,2,6}$), (G) ethanol (P2), (H) butanol (P4), (I) L-lysine, (J) L-threonine, (K) triethylenetetramine (TETA), and (L) spermine. The amount of ZGM used in each synthesis is a molar ratio of x ZGM:1.0 SiO_2, where $x = 0.04$ for spermine, 0.06 for TETA and L-lysine, 0.07 for L-threonine, and 1.5 for all the alcohols. Scale bars equal 1 μm.

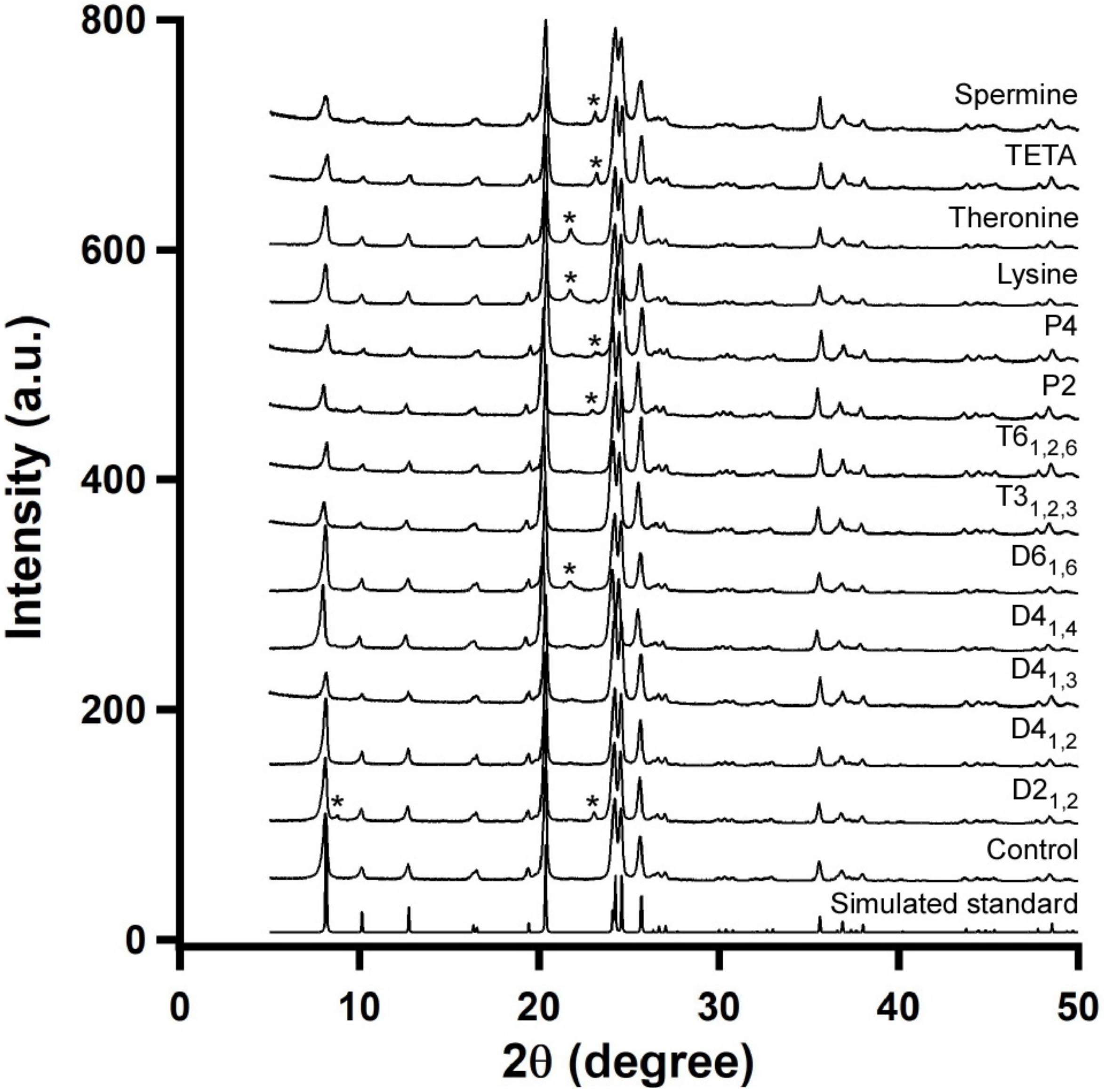

Fig. S3 Powder X-ray diffraction (XRD) patterns of solids extracted from ZSM-22 samples modified using selected ZGMs: ethylene glycol ($D2_{1,2}$), 1,2-butanediol ($D4_{1,2}$), 1,3-butanediol ($D4_{1,3}$), 1,4-butanediol ($D4_{1,4}$), 1,6-hexanediol ($D6_{1,6}$), glycerol ($T3_{1,2,3}$), 1,2,6-hexanetriol ($T6_{1,2,6}$), ethanol (P2), butanol (P4), L-lysine, L-threonine, triethylenetetramine (TETA), and spermine. The amount of ZGM used in each synthesis is a molar ratio of x ZGM:1.0 SiO_2, where $x = 0.04$ for spermine, 0.06 for TETA and L-lysine, 0.07 for L-threonine, and 1.5 for all the alcohols. All the samples examined in this work (including those that are not demonstrated here) possess a major phase structure of **TON** framework, proved by the similarity of their patterns with the simulated **TON** standard pattern. The employment of certain ZGMs could lead to the formation of impurity phases, such as **MTT** and **MEL** zeolites. Peaks corresponding to impurity are marked with an asterisk (*).

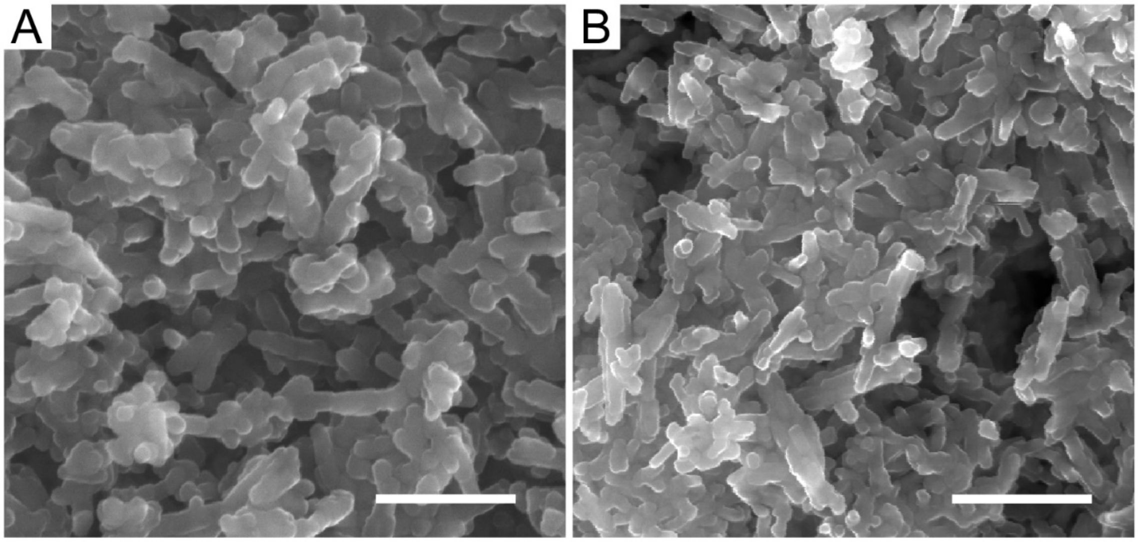

Fig. S4 Electron micrographs of ZSM-22 crystals modified using varying concentrations of triethylenetetramine (TETA), for (A) 0.06 TETA: 1.0 SiO_2 and (B) 0.17 TETA: 1.0 SiO_2. The aspect ratios of samples in panel A and B are 5 ± 2 and 4 ± 2, respectively, both smaller than the aspect ratio of *control* ZSM-22 (i.e., 6 ± 3). Enhanced TETA content does not significantly influence aspect ratio, but indeed reduces the size of the crystals. All scale bars equal 1 μm.

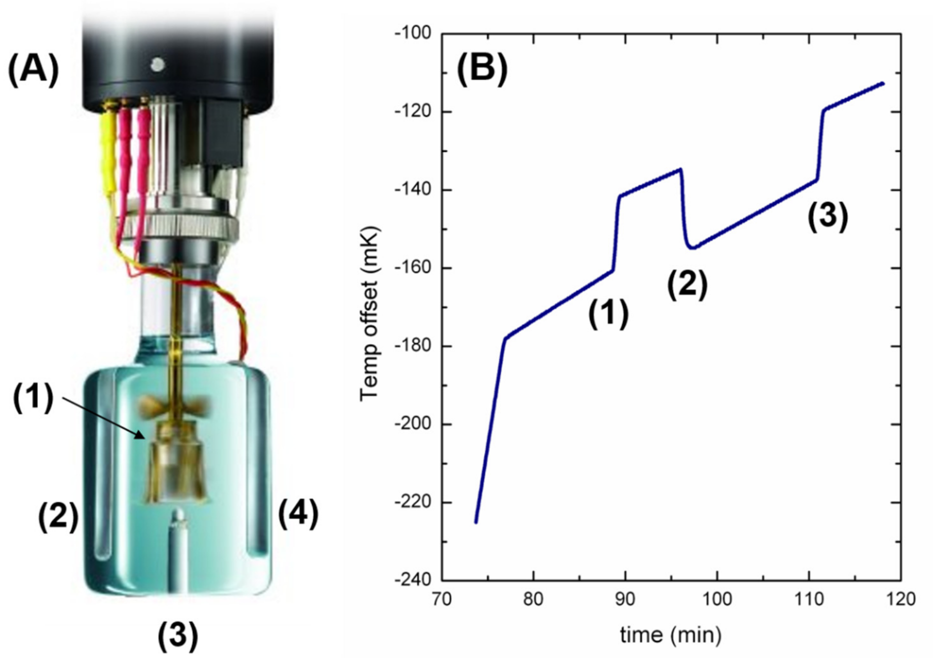

Fig. S5 (A) Picture of the solution calorimeter cell used in a TAM III Precision Calorimeter (TA Instruments, Ogden, UT). The primary pieces of the cell are the sample crushing ampoule (1), calibration heater (2), sapphire tip used to break ampoule (3) and the thermistor which measures the temperature in the cell (4). Enthalpy of solution measurements were conducted at 25.0000 ± 0.0001 C. The zeolite sample (0.1 mg) was placed in a glass ampoule, sealed with a rubber stopper and wax, inserted to the holder of the calorimeter, and placed into a 25 mL reaction vessel filled with solvent. The ampoule was stirred at a rate of 600 rpm throughout the experiment. (B) Mixing of the sample with the solution medium was initiated by breaking the ampoule inside the vessel and the subsequent heat flow was determined by the calorimeter. Calibration was performed by determining the heat capacity of the system twice, before (**1**) and after (**3**) breaking the ampoule where heat flow arises due to wetting of the zeolite by ZGM solution (**2**), by imposing a pulse of 3J power, and measuring the change in temperature. Analysis was performed by SolCal (v1.2, TA Instruments Inc.).

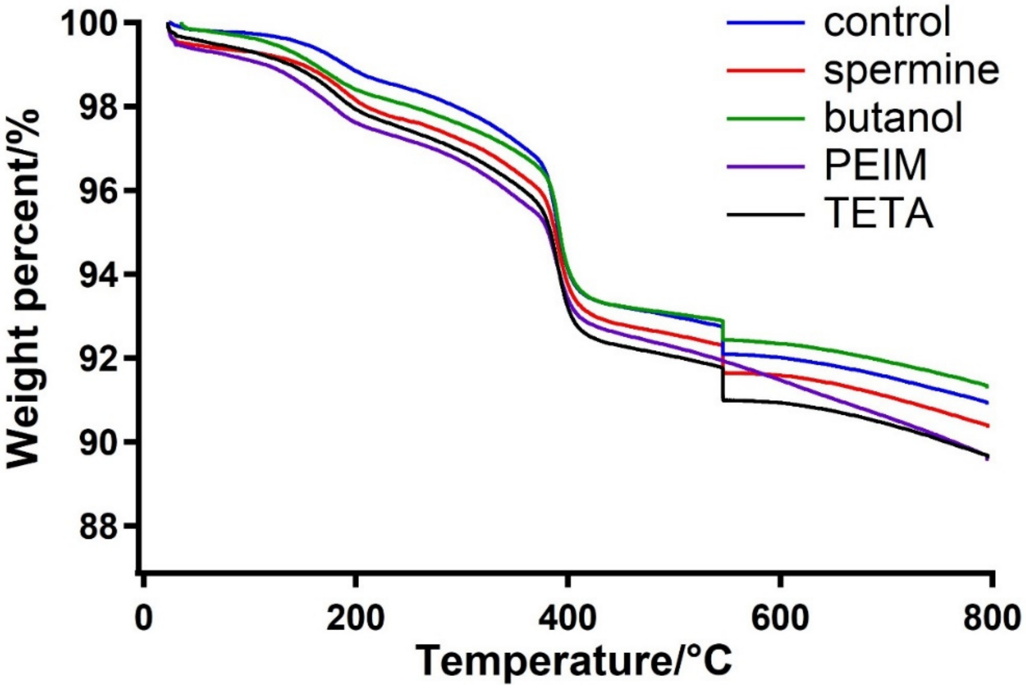

Fig. S6 Thermogravimeric analysis (TGA) analysis of ZSM-22 samples prepared without modifier (control) and with various (macro)molecular modifiers. A maximum weight difference of ca. ±1wt % is observed for different types of modifiers (i.e. amines and alcohols). The quantities of modifiers used in each synthesis were 0.5, 13, 2 and 3 wt% for spermine, butanol, PEIM, and TETA, respectively. Reduction in weight at lower temperature (< 300°C) is attributed to retained water. The weight loss around 400°C is due to the removal of occupied organic structure-directing agent (1,8-diaminooctane) and any residual modifier. A temperature ramp rate of 1°C min^{-1} was used between 25 and 800°C, wherein the system was held at 545°C for 10 h (i.e. the cause of apparent discontinuity in data). Similar analysis of zeolite L samples were reported in previous studies[2, 36] and revealed no appreciable retention of modifiers in the final products.

Movies

Movie S1. Animation showing $D4_{1,3}$ adsorbed onto a S1 site formed by a truncated 6-member ring on the (010) surface of siliceous ZSM-22 (viewed along the c-axis). $D4_{1,2}$ preferentially adsorbs onto S1 sites in a similar manner. Blue dashed lines show hydrogen bonds formed between the diols and surface silanols. Water molecules have been omitted from the visualizations for clarity.

Movie S2. Animation showing $D4_{1,4}$ adsorbed onto a S2 site formed by a truncated 10-member ring on the (010) surface of siliceous ZSM-22 (viewed along the c-axis). Blue dashed lines show hydrogen bonds formed between the diols and surface silanols. Water molecules have been omitted from the visualizations for clarity.

References

1. Teketel, S., W. Skistad, S. Benard, U. Olsbye, K.P. Lillerud, P. Beato, and S. Svelle, *Shape Selectivity in the Conversion of Methanol to Hydrocarbons: The Catalytic Performance of One-Dimensional 10-Ring Zeolites: ZSM-22, ZSM-23, ZSM-48, and EU-1.* ACS Catalysis, 2012. **2**: 26-37.
2. Lupulescu, A.I., M. Kumar, and J.D. Rimer, *A Facile Strategy To Design Zeolite L Crystals with Tunable Morphology and Surface Architecture.* Journal of the American Chemical Society, 2013. **135**: 6608-6617.
3. Hess, B., C. Kutzner, D. van der Spoel, and E. Lindahl, *GROMACS 4: Algorithms for Highly Efficient, Load-Balanced, and Scalable Molecular Simulation.* J Chem Theory Comput, 2008. **4**: 435-47.
4. Wang, J., R.M. Wolf, J.W. Caldwell, P.A. Kollman, and D.A. Case, *Development and testing of a general amber force field.* J Comput Chem, 2004. **25**: 1157-74.
5. Cygan, R.T., J.-J. Liang, and A.G. Kalinichev, *Molecular Models of Hydroxide, Oxyhydroxide, and Clay Phases and the Development of a General Force Field.* The Journal of Physical Chemistry B, 2004. **108**: 1255-1266.
6. Bussi, G., D. Donadio, and M. Parrinello, *Canonical sampling through velocity rescaling.* The Journal of Chemical Physics, 2007. **126**: 014101.
7. Kroutil, O., Z. Chval, A.A. Skelton, and M. Předota, *Computer Simulations of Quartz (101)–Water Interface over a Range of pH Values.* The Journal of Physical Chemistry C, 2015. **119**: 9274-9286.
8. Berendsen, H.J.C., J.R. Grigera, and T.P. Straatsma, *The missing term in effective pair potentials.* The Journal of Physical Chemistry, 1987. **91**: 6269-6271.
9. Parrinello, M. and A. Rahman, *Polymorphic transitions in single crystals: A new molecular dynamics method.* Journal of Applied Physics, 1981. **52**: 7182-7190.
10. Tribello, G.A., M. Bonomi, D. Branduardi, C. Camilloni, and G. Bussi, *PLUMED 2: New feathers for an old bird.* Computer Physics Communications, 2014. **185**: 604-613.
11. Ferguson, A.L., *BayesWHAM: A Bayesian approach for free energy estimation, reweighting, and uncertainty quantification in the weighted histogram analysis method.* Journal of Computational Chemistry, 2017. **38**: 1583-1605.
12. Mallon, E.E., I.J. Babineau, J.I. Kranz, Y. Guefrachi, J.I. Siepmann, A. Bhan, and M. Tsapatsis, *Correlations for Adsorption of Oxygenates onto Zeolites from Aqueous Solutions.* The Journal of Physical Chemistry B, 2011. **115**: 11431-11438.
13. Mallon, E.E., A. Bhan, and M. Tsapatsis, *Driving Forces for Adsorption of Polyols onto Zeolites from Aqueous Solutions.* The Journal of Physical Chemistry B, 2010. **114**: 1939-1945.
14. Mallon, E.E., M.Y. Jeon, M. Navarro, A. Bhan, and M. Tsapatsis, *Probing the Relationship between Silicalite-1 Defects and Polyol Adsorption Properties.* Langmuir, 2013. **29**: 6546-6555.

15. Xiong, R., S.I. Sandler, and D.G. Vlachos, *Molecular Screening of Alcohol and Polyol Adsorption onto MFI-Type Zeolites.* Langmuir, 2012. **28**: 4491-4499.
16. Jamil, A.K. and O. Muraza, *Facile control of nanosized ZSM-22 crystals using dynamic crystallization technique.* Microporous and Mesoporous Materials, 2016. **227**: 16-22.
17. Yeqing, W., C. Zhu, J. Qiu, F. Jiang, X. Meng, X. Wang, C. Lei, Y. Jin, S. Pan, and F.-S. Xiao, *Organotemplate-Free Synthesis of a High-Silica Zeolite with a TON Structure in the Absence of Zeolite Seeds.* European Journal of Inorganic Chemistry, 2016. **2016**: 1364-1368.
18. Hogan, P.J., T.V. Whittam, J.J. Birtill, and A. Stewart, *Synthesis properties and catalytic behaviour of zeolite Nu—10.* Zeolites, 1984. **4**: 275-279.
19. Parker, L.M. and D.M. Bibby, *Synthesis and some properties of two novel zeolites, KZ-1 and KZ-2.* Zeolites, 1983. **3**: 8-11.
20. Araya, A. and B.M. Lowe, *Synthesis and characterization of zeolite Nu—10.* Zeolites, 1984. **4**: 280-286.
21. Asensi, M.A., A. Corma, A. Martínez, M. Derewinski, J. Krysciak, and S.S. Tamhankar, *Isomorphous substitution in ZSM-22 zeolite. The role of zeolite acidity and crystal size during the skeletal isomerization of n-butene.* Applied Catalysis A: General, 1998. **174**: 163-175.
22. Ernst, S., J. Weitkamp, J.A. Martens, and P.A. Jacobs, *Synthesis and shape-selective properties of ZSM-22.* Applied Catalysis, 1989. **48**: 137-148.
23. Olson, D.H., R.B. Calvert, and E.W. Valyocsik, *A process for isomerizing xylenes*. 1984, Google Patents.
24. Jamil, A.K., O. Muraza, M. Sanhoob, T. Tago, H. Konno, Y. Nakasaka, and T. Masuda, *Controlling naphtha cracking using nanosized TON zeolite synthesized in the presence of polyoxyethylene surfactant.* Journal of Analytical and Applied Pyrolysis, 2014. **110**: 338-345.
25. Lowe, B.M. and A. Araya, *Zeolite synthesis*. 1983, Google Patents.
26. Wang, Y., X. Wang, Q. Wu, X. Meng, Y. Jin, X. Zhou, and F.-S. Xiao, *Seed-directed and organotemplate-free synthesis of TON zeolite.* Catalysis Today, 2014. **226**: 103-108.
27. Valyocsik, E.W., *Synthesis of zeolite ZSM-22 with a heterocyclic organic compound*. 1984, Google Patents.
28. Ball, W.J., S.A.I. Barri, and D. Young, *Method of preparing crystalline aluminosilicates*. 1985, Google Patents.
29. Gaona-Gómez, A. and C.-H. Cheng, *Modification of zeolite L (LTL) morphology using diols, (OH)2(CH2)2n+2On (n=0, 1, and 2).* Microporous and Mesoporous Materials, 2012. **153**: 227-235.
30. Larlus, O. and V.P. Valtchev, *Crystal Morphology Control of LTL-Type Zeolite Crystals.* Chemistry of Materials, 2004. **16**: 3381-3389.
31. Megelski, S. and G. Calzaferri, *Tuning the Size and Shape of Zeolite L-Based Inorganic–Organic Host–Guest Composites for Optical Antenna Systems.* 2001. **11**: 277-286.
32. Trakarnroek, S., S. Jongpatiwut, T. Rirksomboon, S. Osuwan, and D.E. Resasco, *n-Octane aromatization over Pt/KL of varying morphology and channel lengths.* Applied Catalysis A: General, 2006. **313**: 189-199.
33. Huo, Q., T. Dou, Z. Zhao, and H. Pan, *Synthesis and application of a novel mesoporous zeolite L in the catalyst for the HDS of FCC gasoline.* Applied Catalysis A: General, 2010. **381**: 101-108.
34. Jentoft, R.E., M. Tsapatsis, M.E. Davis, and B.C. Gates, *Platinum Clusters Supported in Zeolite LTL: Influence of Catalyst Morphology on Performance inn-Hexane Reforming.* Journal of Catalysis, 1998. **179**: 565-580.
35. Itani, L., K.N. Bozhilov, G. Clet, L. Delmotte, and V. Valtchev, *Factors That Control Zeolite L Crystal Size.* 2011. **17**: 2199-2210.
36. Li, R., A. Smolyakova, G. Maayan, and J.D. Rimer, *Designed Peptoids as Tunable Modifiers of Zeolite Crystallization.* Chemistry of Materials, 2017. **29**: 9536-9546.